UCRL-9378

Cy 2

UNIVERSITY OF CALIFORNIA

Ernest O. Lawrence Radiation Laboratory

TWO-WEEK LOAN COPY

This is a Library Circulating Copy which may be borrowed for two weeks. For a personal retention copy, call Tech. Info. Division, Ext. 5545

BERKELEY, CALIFORNIA

Cy. 2

DISCLAIMER

This document was prepared as an account of work sponsored by the United States Government. While this document is believed to contain correct information, neither the United States Government nor any agency thereof, nor the Regents of the University of California, nor any of their employees, makes any warranty, express or implied, or assumes any legal responsibility for the accuracy, completeness, or usefulness of any information, apparatus, product, or process disclosed, or represents that its use would not infringe privately owned rights. Reference herein to any specific commercial product, process, or service by its trade name, trademark, manufacturer, or otherwise, does not necessarily constitute or imply its endorsement, recommendation, or favoring by the United States Government or any agency thereof, or the Regents of the University of California. The views and opinions of authors expressed herein do not necessarily state or reflect those of the United States Government or any agency thereof or the Regents of the University of California.

UCRL-9378

UNIVERSITY OF CALIFORNIA

Lawrence Radiation Laboratory
Berkeley, California

Contract No. W-7405-eng-48

COLLISION MECHANICS IN CROSSED MAXWELLIAN MOLECULAR BEAMS

Dudley R. Herschbach

and

Sheldon Datz and Ellison H. Taylor

August 1960

UCRL 9378

COLLISION MECHANICS IN CROSSED MAXWELLIAN MOLECULAR BEAMS

Dudley R. Herschbach
Department of Chemistry and Lawrence Radiation Laboratory, University of California,*
Berkeley 4, California

and

Sheldon Datz and Ellison H. Taylor
Chemistry Division, Oak Ridge National Laboratory†
Oak Ridge, Tennessee

Abstract

A general treatment of the mechanics of collision between two Maxwellian molecular beams is described. A method for averaging over the velocity distributions of beams colliding at any angle is developed and used to calculate the distribution of collision energies, the elastic and reactive collision rates, and the angular distribution of relative velocity and center of mass vectors. The treatment applies to any reaction cross section which can be expressed as a step function multiplied by a linear combination of powers of the relative energy. The effect of recoil momentum relative to the center of mass on the direction of the product observed in the laboratory system is discussed. Comparison is made with some experimental data for the $K + HBr \longrightarrow H + KBr$ crossed beam reaction.

---

* Support of this work received from the Alfred P. Sloan Foundation and the U.S. Atomic Energy Commission is gratefully acknowledged.

† Operated by Union Carbide Nuclear Corporation for the U.S. Atomic Energy Commission.

The interpretation of chemical kinetics experiments ordinarily requires knowledge of the collision rate between molecules as a function of energy. For a gas mixture, the Arrhenius equation derived from the Maxwell-Boltzmann distribution of velocities is usually an adequate approximation. Recent interest in studying reactions between crossed molecular beams[1,2] raises the need for a comparable expression for this arrangement. In this case, there is also the possibility of observing the angular distribution of the reaction products, and therefore the necessity of calculating the distribution to be expected on various assumptions. Although the use of monoenergetic beams would simplify somewhat the interpretation of results, practical limitations make the use of Maxwellian beams mandatory for many experiments, as the decrease in density accompanying the energy selection can only be tolerated for a relatively small class of reactions in which the collision yield or the detection efficiency for reactants and products is unusually high.

In this type of experiment the two most directly observable quantities are the reactive collision yield, defined as the integrated number of reactive collisions divided by the total collision number, and the angular distribution of products. A rigorous analysis would require a quantum mechanical description of the energy states of pairs of colliding molecules. However, a reasonable starting point is a general formulation in which the dependence of reaction probability on internal energy states is included in a cross-section term and the equivalent

of the classical Arrhenius picture is fully developed for crossed Maxwellian beams. This description may then serve as a basis for a stochastic comparison of detailed collision mechanisms with observed results.

1. Collision Rate in Crossed Beams

The flux distribution of velocities in an effusive beam is given by[3]

$$dI/I_0 = 2(v^3/\alpha^3)\exp(-v^2/\alpha^2)\,d(v/\alpha) \qquad (1)$$

where I_0 is the total flux in molecules/cm^2/sec and $\alpha = (2RT/M)^{1/2}$ is the most probable molecular velocity in the source. However, in order to calculate the number of collisions of a specified nature between molecules in each of two intersecting beams, we have to consider elements of volume $\mathcal{V}$ in each beam moving toward each other, where $\mathcal{V}$ is equal to the volume of intersection of the two beams. Thus the velocity distribution which enters the calculation is that for the density of molecules (n per unit volume) within these volume elements,

$$df = dn/n = (4/\pi^{1/2})(v^2/\alpha^2)\exp(-v^2/\alpha^2)\,d(v/\alpha), \qquad (2)$$

rather than the flux distribution. The number of collisions per second in the reaction volume is then given by

$$kn_1n_2\mathcal{V}$$

in terms of the rate constant,

$$k = \iint v\sigma(v)df_1df_2$$

$$= A\int_0^\infty\int_0^\infty v\sigma(v)v_1^2v_2^2\exp[(-v_1^2/\alpha_1^2)+(-v_2^2/\alpha_2^2)]dv_1dv_2 \quad (3)$$

where $A = 16/(\pi\alpha_1^3\alpha_2^3)$ and k is expressed in the usual units of sec^{-1} $(moles/cc)^{-1}$. Here $\sigma(v)$ is the collision cross section for the process of interest and in general is a function of the relative velocity v. It may be remarked that the use of the initial equilibrium velocity distributions in Eq. (3) does not represent an approximation as in the corresponding calculation for a gas mixture,[4] because in the crossed beam experiment the collisions are always between "fresh" reactants.

To carry out the average over the cross section function and angular distribution calculations, it will be most convenient to employ as integration variables in Eq. (3) not the velocities of the beams, v_1 and v_2, but either v and ψ, the magnitude and angle of the relative velocity vector, or c and θ, those of the center-of-mass vector. The necessary transformations are found from simple kinematical relations; these are now reviewed briefly in the course of specifying our notation.

2. Kinematics

Some conventions will be adopted to avoid ambiguities. Let the particles be numbered so that $M_1 \leq M_2$. The initial velocity vector diagram (Fig. 1) is drawn so that $\underset{\sim}{v}_2$ is reached by a counterclockwise rotation from $\underset{\sim}{v}_1$, and the various angles are measured from the direction of the lighter particle, $\underset{\sim}{v}_1$.

The angle of intersection of the beams, γ, may have any value. The initial velocity vectors refer to an asymptotic state far from the scattering center, but for convenience are drawn as if they were just emerging from the scattering center; thus Fig. 1 may be regarded as applying to an idealized encounter in which no interaction whatever occurred.

From the definitions

$$\underset{\sim}{v} = \underset{\sim}{v}_1 - \underset{\sim}{v}_2$$

$$M\underset{\sim}{c} = M_1\underset{\sim}{v}_1 + M_2\underset{\sim}{v}_2$$

$$M = M_1 + M_2 ,$$

there follow the relations

$$v \cos \psi = v_1 - v_2 \cos \gamma \tag{4}$$

$$v \sin \psi = v_2 \sin \gamma$$

$$Mc \cos \theta = M_1 v_1 + M_2 v_2 \cos \gamma$$

$$Mc \sin \theta = M_2 v_2 \sin \gamma .$$

The angles vary over the ranges

$$0 \leq \psi \leq \pi - \gamma , \tag{5}$$

$$0 \leq \theta \leq \gamma .$$

The transformation equations we shall need are:

$$v_1 = \frac{v \sin (\gamma+\psi)}{\sin \gamma} = \frac{Mc \sin (\gamma-\theta)}{M_1 \sin \gamma} \tag{6}$$

$$v_2 = \frac{v \sin \psi}{\sin \gamma} = \frac{Mc \sin \theta}{M_2 \sin \gamma}$$

$$dv_1 dv_2 = -\ (v/\sin\gamma)\ dv d\psi \tag{7}$$

$$d\psi = (m^2/M_1 M_2)\ d\theta \tag{8}$$

and

$$(v_1^2/\alpha_1^2) + (v_2^2/\alpha_2^2) = v^2/\alpha^2\ . \tag{9}$$

The trivial cases $\gamma = 0$ and $\gamma = \pi$ are excluded.

The quantities m and α introduced here may be regarded as effective mass and velocity parameters, respectively. Their limiting values are constants:

$$m \longrightarrow M_1 \text{ and } \alpha \longrightarrow \alpha_1$$

as $\psi \longrightarrow \theta \longrightarrow 0$;

$$m \longrightarrow M_2 \text{ and } \alpha \longrightarrow \alpha_2$$

as $\psi \longrightarrow \pi - \gamma$ and $\theta \longrightarrow \gamma$. However, the general definitions are angle dependent:

$$m^2 \sin^2\gamma = [M_1^2 \sin^2(\gamma+\psi) + 2M_1 M_2 \cos\gamma \sin(\gamma+\psi)\sin\psi + M_2^2 \sin^2\psi]$$

$$m^{-2}\sin^2\gamma = \left[\frac{\sin^2(\gamma-\theta)}{M_1^2} - \frac{2\cos\gamma\sin(\gamma-\theta)\sin\theta}{M_1 M_2} + \frac{\sin^2\theta}{M_2^2}\right] \tag{10}$$

also, $mv = Mc$.

$$\alpha^2 = \sin^2\gamma\left[\frac{\sin^2(\gamma+\psi)}{\alpha_1^2} + \frac{\sin^2\psi}{\alpha_2^2}\right]^{-1} \tag{11}$$

$$= \frac{\sin^2\gamma}{m^2}\left[\frac{\sin^2(\gamma-\theta)}{M_1^2\alpha_1^2} + \frac{\sin^2\theta}{M_2^2\alpha_2^2}\right]^{-1}$$

3. Method of Calculation

We may now transform Eq. (3) by means of (6) and (7) to obtain

$$k = (A/\sin^5\gamma) \int_0^\infty \int_0^{\pi-\gamma} \sin^2(\gamma+\psi)\sin^2\psi v^6\sigma(v)\exp(-v^2/\alpha^2)dvd\psi \tag{12}$$

The integral over v may be evaluated as a Laplace transform

$$G(p) = \int_0^\infty f(t)e^{-pt}dt, \tag{13}$$

just as in the treatment of collisions in a gas mixture.[5,6] Here $t = v^2$, $p = 1/\alpha^2$, and $f(t) = (\frac{1}{2}A/\sin^5\gamma)t^{5/2}\sigma(t^{1/2})$.

In addition to the rate constant k itself we wish to calculate angular distributions. The distribution of directions of the relative velocity vector is obtained by merely omitting the integration over ψ in Eq. (12).

$$\begin{aligned} \mathcal{P}(\psi) &= dk/d\psi \\ &= \sin^2(\gamma+\psi)\sin^2\psi\, G(1/\alpha^2) . \end{aligned} \tag{14}$$

This may be converted to the angular distribution of centroids by use of the transformations found in Eqs. (6) and (8).

$$\begin{aligned} \mathcal{P}(\theta) &= dk/d\theta = (dk/d\psi)(d\psi/d\theta) \\ &= \sin^2(\gamma-\theta)\sin^2\theta(m^6/M_1^3M_2^3)\, G(1/\alpha^2) \end{aligned} \tag{15}$$

Returning now to Eq. (12), we note that the remaining integration may be carried out over either ψ or θ, and thus the rate constant is given by

$$k = \int_0^{\pi-\gamma} \mathcal{P}(\psi)d\psi = \int_0^{\gamma} \mathcal{P}(\theta)d\theta \ . \tag{16}$$

The integration may not be tractable by analytic means, but a graphical integration is appropriate, as one will usually want to prepare a plot of $\mathcal{P}(\psi)$ or $\mathcal{P}(\theta)$ anyway.

Out of all collisions, the number of those which satisfy various presumed conditions can be found by introducing these conditions into the cross-section $\sigma(v)$ in Eq. (12). A comparison of the collision yield thus calculated with experiment will indicate the degree to which the assumed conditions approach reality, and the whole collisional treatment developed here is simply a framework in which to carry out such comparisons. As yet, we have placed no restrictions on the form of $\sigma(v)$ except that it should have a Laplace transform. In practice, it is sufficient to restrict attention to some convenient functional forms for $\sigma(v)$ if these have enough flexibility to represent the main features of the processes considered.

4. Averages Over Cross Sections for Elastic and Reactive Collisions

The collision yield is defined by

$$k_r/k_t = \int_0^{\gamma} \mathcal{P}_r(\theta)d\theta / \int_0^{\gamma} \mathcal{P}_t(\theta)d\theta \ , \tag{17}$$

the ratio of the reactive collision rate to the total collision rate. Since very small deflections will remove a molecule from the beam, the cross-section for elastic scattering as measured in molecular beam experiments is very large (800 A^2,

for K + HBr, for example). Thus elastic scattering gives a much larger contribution to the total collision cross section than does reactive scattering, and in Eq. (17) we may replace k_t by the rate of elastic collisions.

The cross section for elastic scattering has only a weak dependence on relative velocity, and it is an adequate approximation to represent it by a constant average value, σ_e, which may be taken outside the integral in Eq. (12). The integration over v in Eq. (13) then yields

$$G_e(1/\alpha^2) = (15/\pi^{1/2}\sin^5\gamma)(\alpha^7/\alpha_1^3\alpha_2^3)\sigma_e \tag{18}$$

The angular distributions $\mathcal{P}_e(\psi)$, $\mathcal{P}_e(\theta)$, and the rate constant k_e for elastic scattering may now be obtained from Eqs. (14)-(16).

In evaluating the reactive collision rate, we shall use several cross section functions. We first consider the simple cross sections that accord with two traditional models for reaction. Model "A" assumes that $\sigma(v)$ is a step function with respect to relative energy and impact parameter and is independent of orientation and internal excitation. That is,

$$\begin{aligned} \sigma(v) &= 0, \quad v < v^* \\ &= \sigma_r, \quad v > v^*, \end{aligned} \tag{19a}$$

where σ_r is a constant and v^* is related to the activation energy E^* and reduced mass $\mu = M_1M_2/M$ by

$$E^* = \tfrac{1}{2}\mu(v^*)^2 .$$

The integration over this cross section in Eq. (12) differs from the elastic case only because the lower limit is now v^* instead of zero. Model "B" assumes further that only the component of relative velocity along the line of centers at impact is effective. The cross section above v^* is then not constant, and takes the form[7]

$$\sigma(v) = \sigma_r[1 - (v^*/v)^2] \ . \tag{19b}$$

A third cross section function, "Model C", is suggested by the calculations of Wall, Hiller, and Mazur on the $H + H_2$ reaction.[8] They found a reaction probability which decreased rapidly with increasing energy above the threshold (see the insert in Fig. 2); the corresponding cross section is approximately

$$\begin{aligned} \sigma(v) &= 0, \ v < v^* \\ &= \sigma_r(v^*/v)^{20}, \ v > v^* \ . \end{aligned} \tag{19c}$$

A more general functional form which can be readily treated consists of a step function multiplied by any linear combination of powers of the relative energy:

$$\begin{aligned} \sigma(E) &= 0, \ E < E^* \\ &= \sigma_r \sum_n c_n \ (E^*/E)^n, \ E > E^* \end{aligned} \tag{20}$$

The exponents $\underline{n}$ may be positive or negative intergers; the constants c_n are dimensionless and could be taken as adjustable parameters. Eq. (20) includes models A, B, C as special cases: for A, $c_0 = 1$; for B, $c_0 = 1$, $c_1 = 1$; for C, $c_{10} = 1$ are the nonzero coefficients.

The results for any reaction cross section that can be represented by Eq. (20) take the following simple form:

$$G_r(1/\alpha^2) = (\sigma_r/\sigma_e)\, G_e(1/\alpha^2)\, F_r(z) \tag{21}$$

and

$$\mathcal{P}_r(\theta) = (\sigma_r/\sigma_e)\, \mathcal{P}_e(\theta)\, F_r(z), \tag{22}$$

where $F_r(z)$ is a function of the dimensionless ratio

$$z = v^*/\alpha\ . \tag{23}$$

As seen from Eq. (11), z depends on the angle, and on the masses and temperatures of the beam molecules as well as the activation energy. The functions $F_r(z)$ are attenuation factors that modify the result for elastic scattering to take account of the premium placed on relative energy by the reaction cross section. For all cross sections of the form of Eq. (20), the $F_r(z)$ functions can be expressed in terms of the probability integral and its derivative,

$$H(z) = (2/\pi^{1/2}) \int_0^z e^{-t^2} dt,$$

$$H'(z) = (2/\pi^{1/2})\, e^{-z^2},$$

for which extensive tables are available.[9] It is only necessary to outline the calculation of the function $F_m(z)$ corresponding to a single term of Eq. (20), since the general result may be constructed as a linear combination,

$$F_r(z) = \sum_m c_m F_m(z)\ . \tag{24}$$

We have, from Eqs. (12) and (21),

$$F_n(z) = \int_{v^*}^{\infty} (v^*/v)^{2n} v^6 e^{-v^2/\alpha^2} dv \Big/ \int_0^{\infty} v^6 e^{-v^2/\alpha^2} dv \ , \tag{25}$$

and use of the Laplace transform tables gives[10]

$$F_n(z) = z^{2n}\Gamma(-n + \tfrac{7}{2}; z^2)/\Gamma(\tfrac{7}{2}) \tag{26}$$

where

$$\Gamma(a,x) = \int_x^{\infty} e^{-t} t^{a-1} dt \tag{27}$$

is the incomplete gamma function.[11] The integration is trivial for the case $n = 3$, and yields

$$F_3(z) = (8z^6/15)[1 - H(z)].$$

This is all that is needed, however, for the other functions are readily generated by use of a recurrence relation

$$(n - \tfrac{5}{2})F_{n+1}(z) + z^2 F_n(z) - 4(4/15)z^7 H'(z) = 0, \tag{28}$$

which is established from Eq. (26) by integrating (27) by parts. The results for models A and B, for example, are found to be

$$F_A(z) = [1 - H(z)] + z[1 + (2/3)z^2 + (4/15)z^4]H'(z) \tag{29a}$$

and

$$F_B(z) = (1 - \tfrac{2}{5}z^2)[1 - H(z)] + z[1 + (4/15)z^2]H'(z). \tag{29b}$$

In Fig. 2 these are compared with the functions for various values of n, including model C ($n = 10$ case). Table I gives F_A ($n = 0$ case) and F_B($n = 0$ minus $n = 1$ case) and the function

$(4/15)z^7H'(z)$, so that any of the $F_n(z)$ functions may be obtained from the table by use of Eq. (28).

5. Procedure for Analysis of Data

Our results may now be summarized in terms of a stepwise procedure for the analysis of experiments on the basis of models such as those considered here. Two parameters, the activation energy E^* and the ratio σ_r/σ_e, are to be fitted to the data; some of the coefficients c_n in Eq. (20) could also be taken as adjustable parameters.

A. Angular distribution of centroids for elastic collisions. $\mathcal{P}_e(\theta)$ is calculated from Eqs. (15) and (18). Aside from the scale factor σ_e, the distribution depends only on the beam masses, temperatures, and the angle of intersection, γ. In Fig. 3, distributions are plotted for several angles of intersection. The beams in this example (which corresponds to the conditions listed in Table II) have about the same average momenta; thus the centroids peak near $\theta = 45°$ for perpendicular beams. For an acute intersection, the distribution shifts to favor $\theta = 0$, which would be the only accessible angle when $\gamma = 0$ and the beams merge. On the other hand, if the beams intersect at a sufficiently obtuse angle, the distribution becomes bimodal, since in collisions between fast molecules of beam one and slow molecules of beam two, the center of mass vector lies nearer to beam one, and vice versa. The relative height of the forward and backward peaks again reflects the ratio of the average momenta of the beams.

B. Dependence of z^2 on the centroid angle, θ.

From Eqs. (6) and (11), one finds that

$$z^2 = (E^*/RT_1)(E_1/E) + (E^*/RT_2)(E_2/E) \tag{30}$$

The ratios of the energies of the beams to their relative energy, E_1/E and E_2/E, depend only on the masses and on θ:

$$\begin{aligned} E_1 &= \frac{m^2}{\mu M_1} \frac{\sin^2(\gamma-\theta)}{\sin^2\gamma} E \\ E_2 &= \frac{m^2}{\mu M_2} \frac{\sin^2\theta}{\sin^2\gamma} E \end{aligned} \tag{31}$$

Thus, after preparing a graph of these ratios, one may readily read off z^2 as a function of θ for any set of values of T_1, T_2, and E^*.

According to Eq. (22), it is only the variation of z^2 with θ that enables the velocity dependence of the cross section to influence the form of the angular distribution of centroids.[12] Fig. 4 shows the variation of z^2 over the range of θ for beams colliding at various angles, again for the example of Table II. As seen from the limiting values,

$$\begin{aligned} z^2 &\rightarrow \left(1 + \frac{M_1}{M_2}\right) \frac{E^*}{RT_1}, \text{ as } \theta \rightarrow 0; \\ z^2 &\rightarrow \left(1 + \frac{M_2}{M_1}\right) \frac{E^*}{RT_2}, \text{ as } \theta \rightarrow \gamma, \end{aligned} \tag{32}$$

which are the same for beams intersecting at any angle, the lowest values of z^2 occur near the beam having the higher average velocity. Adjusting the value of E^* merely changes the vertical scale of the figure. The drastic changes in form of the curves for various angles of intersection are primarily due to a simple kinematical effect: for given velocities of the beams, the relative velocity at an acute intersection is much less than that at an obtuse intersection (see the

velocity vector diagrams shown as inserts in Fig. 4); this difference is magnified in computing z^2, since z^2 is a measure of the available relative energy.

C. Attenuation factors. The function $F_r(z)$ corresponding to a given cross section is evaluated by use of Table I and Eqs. (24) and (28). To convert from z to θ as independent variable, one prepares a graph such as Fig. 4; this step differs for each set of experimental conditions (intersection angle, beam temperatures, and masses) and for each value of the activation energy that is to be considered. The attenuation factor of Model B is shown as a function of θ in Fig. 5a, which has been derived from Figs. 2 and 4. Results for Model A are qualitatively similar. For both of these models, changing E* merely shifts the curves about without much altering their shape. However, as seen in Fig. 2, the attenuation factor is not a monotonic function of z for cross sections such as that of Model C, which decreases with increasing energy above the threshold. Accordingly, if the range of z involved includes the hump shown in Fig. 2, the angular dependence of the attenuation factor will rapidly change character as E* is adjusted (or as an equivalent change in beam temperatures is made). This is illustrated in Fig. 5b. It will be noticed that for sufficiently large values of E*, F_C has an angular dependence similar to that of F_B (because they become nearly parallel functions of z when z is large), so that both favor the faster beam, i.e., low angles. For small values of E*, low angles are still favored by F_B whereas large angles are favored by F_C.

D. Angular distribution of centroids for reactive collisions. According to Eq. (22), $\mathcal{P}_r(\theta)$ is now obtained by multiplying the attenuation factor into the distribution of centroids for elastic collisions. Fig. 6 gives some typical results derived in this way from Figs. 3 and 5. The various special features discussed in connection with Figs. 3, 4, and 5 all appear superimposed in Fig. 6. In particular, the extent of the shifting and skewing of the curves in Fig. 6a, as compared with Fig. 3, differs considerably for different angles of intersection, the attenuation being much more pronounced for acute intersections. Variation of the intersection angle would appear to be especially helpful in attempting to choose between reaction models: for example, under the conditions of Fig. 6a, the ratio of the maxima in the angular distribution for the $\gamma = 30°$ and the $\gamma = 150°$ cases is nearly twice as large for Model A as for Model B.

The relation of the angular distribution of centroids to that of the product fragments will be considered in Sec. 6. If the detected product is heavy and the energy liberated in the reaction is small, as for the K + HBr → H + KBr reaction, the distribution of the product will be quite close to the centroid distribution.[13] In such cases, an estimate of the activation energy may be obtained in the course of comparing the observed distribution with the $\mathcal{P}_r(\theta)$ calculated for various values of E* (see Fig. 9), although a more precise determination can usually be made from the temperature variation of the collision yield.

The angular distribution of initial relative velocity vectors, $\mathcal{P}_r(\psi)$, may be calculated by an entirely analogous

procedure, using Eq. (14) and

$$\mathcal{P}_r(\psi) = (\sigma_r/\sigma_e)\mathcal{P}_e(\psi)F_r(z)$$

However, since the relative velocity is a constant of the motion only for elastic collisions, $\mathcal{P}_r(\psi)$ is not as generally useful for comparison with the product distribution as is the centroid distribution.

E. Rate constants, collision yield, and determination of parameters. As shown in Eq. (16), the area under a curve in Fig. 3 or 6 gives the corresponding rate constant. In the general case a numerical integration is required. Analytical expressions for some special cases are obtained in the Appendix; however, it is found that even for these cases the use of Simpson's method or a planimeter is more rapid.

The calculated collision yield is the ratio of rate constants for elastic and reactive scattering, k_r/k_e. In the present treatment, this is proportional to σ_r/σ_e and otherwise depends only on E^*, for a given reaction model and a particular choice of beam temperatures and intersection angle. Graphs of k_r/k_e versus E^* for the various reaction models resemble the curves of $F_r(z)$ versus z^2 in Fig. 2. This may be understood from the limiting cases discussed in the Appendix. The variation of rate constants with intersection angle is shown in Fig. 7. The decrease in collision rate which occurs for acute intersections varies considerably with the reaction model. (The model designated here as A - B refers to the $n = 1$ case in Fig. 2.)

In reference 1, a procedure is described for evaluating E^* and σ_r/σ_e from the temperature variation of the collision

yield. Ratios of observed collision yields for pairs of experiments with different reactant temperatures are compared with calculated ratios for various choices of E*. It is assumed that σ_r/σ_e is independent of temperature so that this parameter cancels from the ratios. It is then adjusted to fit the magnitude of the collision yields after E* is obtained from the ratios.

As discussed in Sec. 7, the available data may be satisfactorily analyzed on this basis, although one finds that with suitable adjustments of the parameters the various reaction models give practically equivalent agreement with experiment (see Table III). This occurs because E* is large enough to make the relevant region of Fig. 2 that in which the $F_r(z)$ functions are practically parallel, so a suitable shift of the scale of z^2 (change of E*) makes the various attenuation factors almost the same. The present calculations show that the analysis would be much more sensitive to the model used if the intersection angle as well as the beam temperatures were varied, as then the attenuation factors could not be brought into such close superposition by a simple scale change. No data of this kind are yet available.

6. Angular Distribution of Reaction Products; Effect of Recoil Momentum

A unique feature of molecular beam methods for reaction studies is the possibility of observing the angular distribution of products. It is convenient to divide the description of the angular distribution into two parts. The

first is $\mathcal{P}_r(\theta)$, the distribution of center-of-mass directions in the laboratory system, which is also the distribution of the initial directions of motion of the collision complex. As discussed in the foregoing, $\mathcal{P}_r(\theta)$ is a function only of the initial kinetic energy distribution and the velocity dependence of the reaction cross section. The second part is the distribution in direction and magnitude of the momenta of the products relative to a coordinate system traveling with the center-of-mass (CM system). The magnitude of any given momentum vector in this CM system is a function of the initial relative energy and the energy released in the reaction. The directions of momentum vectors in the CM system will be anisotropic if the collision efficiency is different for different orientations and if the lifetime of the complex is short compared to its rotational period. The anisotropy can be observed in the laboratory system because the experimental arrangement polarizes the direction of relative motion with respect to the direction of the center-of-mass vector.

The distribution of center-of-mass directions can be combined with the distribution of product in the CM system to give the distribution of product in the laboratory system, but the complexity of the result poses a lengthy problem even for numerical integration. We have therefore considered it expedient to limit the quantitative development initially to the more tractable first stage of the description, given by $\mathcal{P}_r(\theta)$. The perturbations imposed on this distribution by the break-up of the complex can be examined under various assumptions about the reaction mechanism, and results compared

with experiment to indicate qualitatively the range and form of the trial parameters to be used in a complete calculation of the angular distribution of products.

In the dissociation of a collision complex in a reaction of the type

$$M_1 + M_2 \longrightarrow M_3 + M_4,$$

the magnitude of the velocity, v_3', imparted to a product fragment in the CM system is calculable from energy balance.

$$v_3' = \left\{\frac{2(E + Q)}{M_3[1 + (M_3/M_4)]}\right\}^{1/2}, \tag{33}$$

where E is the initial relative energy in the collision of the reactants and Q is the energy converted from internal degrees of freedom (rotational, vibrational, or electronic) to relative kinetic energy of the products. Thus Q is determined by the difference in zero point energy of the reactants and products, ΔD_o^o, and the difference in internal excitation energy of the reactants, U_r, and the products, U_p:

$$Q = \Delta D_o^o + U_p - U_r. \tag{34}$$

Q is zero, positive, or negative, according as the collision is elastic, exothermic, or endothermic, respectively.

As the vector $\underset{\sim}{v}_3'$ may point in any direction in the CM system, its possible directions generate a sphere about the tip of the center-of-mass vector, as indicated in Fig. 8.

The velocity of the product in the laboratory system, $\underset{\sim}{v}_3$, is the vector sum of its recoil velocity, $\underset{\sim}{v}_3'$, in the CM system and the velocity of the centroid in the laboratory system, $\underset{\sim}{c}$. Consequently, for any given recoil angle ϕ_3' in the CM system, the possible directions of velocity vectors in the laboratory

system generate a cone of half angle ϕ_3 about the original centroid direction, where

$$\tan \phi_3 = \sin \phi_3' / (x_3 + \cos \phi_3'), \tag{35}$$

and x_3 is the ratio of the speed of the centroid in the laboratory system to that of M_3 in the CM system,

$$x_3 = \frac{c}{v_3'} = \left[\frac{M_3}{M_4} \frac{E_c}{E + Q} \right]^{1/2} . \tag{36}$$

where E_c is the translational energy of the center-of-mass.[14] Similar equations obtain for the other product, M_4.

Whenever $x_3 > 1$, as in Fig. 8, the laboratory distribution of the product M_3 will be confined to a forward cone about the centroid direction, regardless of the form of the distribution in the CM system. The maximum possible angular displacement of the product direction from the centroid direction in this case is

$$\phi_3^{max} = \sin^{-1}(1/x_3) . \tag{37}$$

Thus, from Eqs. (34) and (36) it is seen that for given initial conditions (beam velocities and angle of intersection), the unknown parameter which determines the maximum possible broadening due to recoil is the internal excitation of the products, since in general ΔD_o^o is known and U_r may be estimated from the source temperatures of the reactants.

The consequences of this effect recommend, for the first crossed beam studies, reactions with values of x_3 well above unity; that is, reactions in which the detected product is relatively heavy and the Q-value is small, such as K + HBr $\rightarrow$ H + KBr. In such cases,

a considerable enhancement of intensity can be obtained, since the solid angle accessible to M_3 in the laboratory system is reduced to

$$4\pi \sin^2 \left(\frac{1}{2}\phi_3^{max}\right) \tag{38}$$

steradians (see Table II for examples), whereas when $x_3 < 1$ the product M_3 could scatter into 4π steradians. For sufficiently large x_3, the recoil broadening given by Eq. (37) will be quite small, less than 3° if $x_3 > 20$, and the angular distribution of M_3 must then follow closely the centroid distribution, $\mathcal{P}_r(\theta)$. The radius of the sphere in Fig. 8 will be so shrunken (to less than one-twentieth of c when $x_3 > 20$) that no features of the recoil scattering in the CM system can influence the laboratory distribution under the resolution attainable in practice. The procedures given in Section 5 should then be sufficient for interpretation of the data.

As one retreats from the limit of large x_3, the possible anisotropy in the distribution of recoil angles in the CM system can have a more and more pronounced effect on the laboratory distribution, which is thereby skewed with respect to the one expected from isotopic addition of the recoil to $\mathcal{P}_r(\theta)$. There is the further complication that the degree of anisotropy will have some velocity dependence, and this need have no simple relation to the velocity dependence of the total reaction cross section which entered into the calculation of $\mathcal{P}_r(\theta)$.

Although it is clear that the influence of the three factors determining the contribution of recoil (internal excitation of products, anisotropy of the angular distribution, and the velocity dependence) cannot be untangled by comparing the observed product

distribution with $\mathcal{P}_r(\theta)$, one may hope to find at least qualitative interpretations which are consistent with results from different experiments and with intuition based on knowledge of molecular structure and energetics.[15] In particular, it would appear unlikely that the distribution of recoil angles would typically happen to be such as to prevent attainment of the ϕ^{max} of Eq. (37); thus one might expect that the maximum deviation of the observed distribution from $\mathcal{P}_r(\theta)$ would permit a reliable estimate of the internal excitation of the products to be made.

7. Discussion of the K + HBr ⟶ H + KBr Reaction

Table II summarizes the conditions for one of the experiments reported in Ref. 1; the calculations presented in Figs. 3-9 correspond to these conditions.

The maximum value of Q (which will give the largest possible value of ϕ^{max}_{KBr} for given initial relative energy) occurs for reactions that leave the newly-formed KBr molecule in its lowest internal state. This lies only about 4 kcal/mole below that of HBr.[16] Practically all the HBr molecules are in the ground vibrational state and most have between 0.3-1.2 kcal/mole of rotational energy. Thus $Q \lesssim 5$ kcal/mole, if we allow about 1 kcal/mole for the initial rotational excitation of HBr.

Fig. 6 has been drawn for E = 3 and Q = 5 kcal/mole, and shows $\phi^{max}_{KBr} = 10.2°$ at $\theta = 37.6°$; under these conditions ϕ^{max} varies from 13° at $\theta = 0°$ to 7° at $\theta = 90°$.

The extent to which appreciable internal excitation of the KBr might be expected to shrink the recoil broadening is illustrated in Table II. For a number of exothermic exchange reactions with small activation energies, there is evidence that the newly-formed bond is vibrationally highly excited.[17] Although the exothermicity in these examples is quite large, and the situation may be somewhat different in the present case of a reaction that is almost thermoneutral, these results suggest that most of the reactive collisions may be expected to have Q values near zero or perhaps slightly negative, corresponding to the formation of KBr with about 3-6 kcal/mole of vibrational and rotational energy.

In Fig. 9, the distribution of centroids calculated for Model B is compared with a typical experimental curve. It is seen that the distributions calculated for $E^* = 2.5$ and 3.0 kcal/mole fit reasonably well and are about as close to the KBr distribution as expected from the discussion of Q-values. The sharp decline observed at 20° is not reproduced, and above 60° the calculated curve looks to be too low, but elsewhere it is notable that the experimental curve is broadened only slightly beyond the centroid distribution (especially considering that the beam widths are about 4°).

It is to be emphasized that the interpretation of deviations of the product distribution from $\mathcal{P}_r(\theta)$, as discussed in Sec. 6, must remain somewhat speculative, particularly until further experimental data are available which allow comparisons with other reactions. However, two features indicated by the present

data should be pointed out. First, it appears unlikely that the choice of another reaction model for the calculation of $\mathcal{P}_r(\theta)$ would lead to significantly better agreement in Fig. 9. Model B has been used here because it leads to the conventional form,

$$k_r = \bar{v}\ \sigma_r \exp(-E^*/RT),$$

when applied to a homogeneous gas mixture.[5,7] One might expect, for example, that a cross section of the type of Model C, which decreases with increasing relative energy, would provide an explanation of the abrupt decrease in KBr intensity at low angles. [As seen in Eq. (31), the relative energy is largest at low angles.] Although this would hold if E^* were sufficiently low, it turns out that the temperature variation of the collision yield determined from several other experiments[1] requires one to chose a rather high value of E^*, as shown in Table III. Then one finds that $\mathcal{P}_C(\theta, E^* = 3.97)$ nearly coincides with $\mathcal{P}_B(\theta, E^* = 2.51)$, for the reason given in the general discussion of Sec. 5E. The situation was similar for all of the reaction models we have tried; parameters for several of these are given in Table III.[18,19] For this reaction at least, the centroid distribution can be regarded for practical purposes as experimentally determined from the temperature variation of the collision yield. The second remark is: if we now accept $\mathcal{P}_B(\theta)$ as a fairly accurate approximation to the true centroid distribution, we find in Fig. 9 a tendency for the KBr distribution to be skewed away from the K beam (less KBr at low angles, more at large angles). This implies that in the reactive collisions

the KBr tends to come off to the outside of the path of the center of mass, and the H to the inside, the side away from the incoming K atom. This is evidently what is to be expected if collisions with the Br end of HBr are more often fruitful than other configurations.

Recently Greene, Roberts, and Ross[2] have successfully carried out a crossed beam study of the K + HBr reaction using practically monoenergetic beams. The detailed information which can be obtained from this type of experiment will be extremely valuable; their work has already demonstrated that the conventional interpretation of E^* as a threshold energy is oversimplified, as some KBr was detected from collisions with relative energy as low as 1.4 kcal/mole. We have not been able to make use here of the results so far reported, however, because in this particular experiment the velocity dependence of the collision yield was measured at a fixed laboratory angle. Thus, as the velocity was varied, the observations necessarily corresponded to various recoil angles in the center of mass system. The observed results therefore represent a superposition of the angular dependence and the velocity dependence of the scattering in the CM system. All that can be said at present is that these results are compatible with the previous data.

Acknowledgment

We have enjoyed many helpful discussions with G. W. Trammell and correspondence with F. C. Stafford and P. Toennies.

Appendix. Closed Forms for Special Cases

Analytic expressions for the rate constants considered in Sections 4 and 5 can be obtained in some special cases that will frequently occur in practice.

Collisions of "Fast" and "Slow" Beams

If the most probable velocities in the colliding beams differ greatly ($\alpha_1 \ll \alpha_2$, say), it will be a good approximation to set the relative velocity equal to the velocity of the faster beam, $v \approx v_2$, particularly for the large values of v of interest in reactive collisions. In Eq. (3), the integration over the distribution of velocities in the slower beam may then be carried out separately, so that

$$k = (4\pi^{-1/2}\alpha_2^{-3}) \int_0^\infty v_2^3 \, \sigma(v_2) \exp(-v_2^2/\alpha_2^2) dv_2 \qquad \text{(A1)}$$

This integral has the same form as that for a homogeneous gas. It may be written as a Laplace transform, as in Eq. (13), with

$$k = G(p), \; p = 1/\alpha_2^2 ,$$

$$f(t) = (2\pi^{-1/2}\alpha_2^{-3})t \; \sigma(t^{1/2}) .$$

For a cross section of the form adopted in Eq. (20),

$$k = \Sigma_n c_n k_n , \qquad \text{(A2)}$$

and the tables[10] give

$$k_n = (2/\pi^{1/2})\alpha_2 \sigma_r z^{2n} \Gamma(2-n, z^2) \qquad \text{(A3)}$$

in terms of the gamma function of Eq. (27). For elastic

collisions, $n = 0$ and $z = 0$, this yields

$$k_e = (2/\pi^{1/2})\alpha_2\sigma_e = \bar{v}_2\sigma_e \ , \tag{A4}$$

where $\bar{v}_2$ is the average velocity in the source. When $n = 1$, the result is also simple,

$$k_1 = \bar{v}_2\sigma_r z^2 e^{-z^2}. \tag{A5}$$

Integration of Eq. (A3) by parts gives a recurrence relation

$$(n-1)k_{n+1} + z^2 k_n = z^2 k_1 \ , \tag{A6}$$

from which results for any value of n are readily generated. The rate constants for Models A and B have the familiar form

$$k_A = \bar{v}_2\sigma_r(1+z^2)e^{-z^2}$$

$$k_B = \bar{v}_2\sigma_r e^{-z^2}.$$

However, here

$$z^2 = (v^*/\alpha_2)^2 = (M/M_1)(E^*/RT_2). \tag{A7}$$

The factor $\mu/M_2 = M/M_1$ arises from the idealization that only the motion of M_2 contributes to the relative velocity. Eq. (A3) and derived results are only exact in the limit $\alpha_1/\alpha_2 \rightarrow 0$, but remain accurate within 5% or better up to about $\alpha_1/\alpha_2 \approx 0.1$, when z is greater than unity.

Perpendicular Collisions

For beams intersecting at $\gamma = 90°$, Eq. (12) may be rewritten as

$$k = AD(1/\alpha_1^2)D(1/\alpha_2^2) \int_0^\infty \int_0^{\pi/2} v^2 \sigma(v) \exp[-v^2(p+q\cos 2\psi)] dv d\psi, \tag{A8}$$

as may be seen from inspection of Eq. (11). $D(x)$ is the differential operator, $\partial/\partial x$, and

$$p = \frac{1}{2}\left(\frac{1}{\alpha_1^2} + \frac{1}{\alpha_2^2}\right), \quad q = \frac{1}{2}\left(\frac{1}{\alpha_1^2} - \frac{1}{\alpha_2^2}\right).$$

It is convenient to number the particles so that $\alpha_1 \leq \alpha_2$, to make q a positive quantity. Use of the identity

$$D(1/\alpha_1^2)D(1/\alpha_2^2) = \frac{1}{4}[D^2(p) - D^2(q)],$$

further differential operation, and integration over ψ yield

$$k = \alpha_1^{-3}\alpha_2^{-3}D(-p)[D^2(p) - D^2(q)]G(p,q), \tag{A9}$$

$$G(p,q) = \int_0^\infty e^{-pt} I_0(q,t) t^{-1/2} \sigma(t^{1/2}) dt, \tag{A10}$$

where $t = v^2$, and $I_0(x)$ is the modified Bessel function.[20]

We consider first the case in which the most probable velocities in the two beams are practically equal, $\alpha_1 = \alpha_2$. Here $q = 0$ and $I_0(0) = 1$, so that Eq. (A10) reduces to a standard form.[10] The results obtained are

$$k_e = \bar{v}_2 \sigma_e (15\pi/16) \tag{A11}$$

and

$$k_n = \bar{v}_2 \sigma_r F_n(z) . \tag{A12}$$

Another route to Eq. (A11) is to specialize Eqs. (16) and (18), which gives

$$k_e = \int_0^{\pi/2} \mathcal{P}_e(\theta)d\theta = \bar{v}_2\sigma_e(15\pi/16)$$

Comparing Eqs. (A4) and (A11), one sees that as α_1/α_2 is varied from zero to unity, the collision rate increases by a factor, $15\pi/16$, that represents the integral over the distribution of centroids. Similarly, Eq. (A12) can be obtained directly from (16) and (22), since z is independent of θ when $\alpha_1 = \alpha_2$ and $\gamma = 90°$. Eqs. (A11) and (A12) remain accurate to about 5% even when α_1 and α_2 differ by as much as 20%.

When $0 < \alpha_1/\alpha_2 < 1$, analytic integration of Eq. (A10) is not feasible for the types of reaction cross sections included in Eq. (20). However, if α_1/α_2 is not too close to unity, a good approximation is obtained by keeping just the first term in the asymptotic expansion

$$I_0(x) \sim e^x(2\pi x)^{-1/2}[1 + (1/8x)+\ldots] .$$

With this approximation, one finds

$$k_n = \bar{v}_2\sigma_r z^{2n}[R'\Gamma(2-n,z^2) + R''\Gamma(1-n,z^2)] \tag{A13}$$

where

$$R' = (1-r^2)^{-3/2}$$

$$R'' = -\frac{3}{2}r^2(1-r^2)^{-5/2}$$

and $r = \alpha_1/\alpha_2$. Results for the cases with $n = 0, 1$ are

$$k_0 = k_A = \bar{v}_2\sigma_r e^{-z^2}[R'(1+z^2) + R''] , \tag{A14}$$

$$k_1 = \bar{v}_2\sigma_r z^2 e^{-z^2}[R' + R''e^{z^2}\Gamma(0,z^2)], \tag{A15}$$

and $k_B = k_0 - k_1$, where

$$\Gamma(0,x) = -\,Ei(-x) = \int_x^\infty e^{-t}t^{-1}dt$$

is the exponential integral.[21] Recurrence relations again offer a convenient means to extend the results. Using primes to distinguish the first and second terms of Eq. (A13),

$$k_n = k_n' + k_n'' ,$$

we may write the relations as:

$$(n-1)k_{n+1}' + z^2 k_n' = z^2 k_1' \qquad \text{(A16)}$$

$$n\,k_{n+1}'' + z^2 k_n'' = z^2 k_0'' .$$

The relative error due to the neglect of the second and higher terms in the asymptotic expansion will be less than

$$\frac{1}{8q(v^*)^2} = \frac{r^2}{4z^2(1-r^2)} .$$

Thus Eq. (A13) reduces to the proper limit, Eq. (A3), as $r \to 0$, but becomes invalid in the limit $r \to 1$ and also for elastic collisions, for which $z = 0$. As long as the beams have sufficiently different average velocities, however, Eq. (A13) will be a suitable approximation for most chemical reaction studies: for the K + HBr reaction under the conditions of Table II, the relative error is only about 0.003 at $E^* = 2.5$ kcal/mole. In case r is near unity, the appropriate approximation is Eq. (A12).

For elastic collisions, Eq. (A10) can be integrated in closed form. One ultimately[22] finds

$$G(p,q) = \sigma_e \pi^{1/2} p^{-1/2} {}_2F_1(\tfrac{1}{4},\tfrac{3}{4};1;\zeta)$$

where ${}_2F_1(a,b;c;x)$ is the Gauss hypergeometric function,[23] and

$$\zeta = (q/p)^2 = (1-r^2)^2/(1+r^2)^2 .$$

The rate of elastic collisions is then given by

$$k_e = \bar{v}_2 \sigma_e R''' f(\zeta) \tag{A17}$$

where

$$R''' = \pi r^4 [2/(1+r^2)]^{7/2}$$

and

$$f(\zeta) = (15/8)F + \tfrac{5}{2}(15\zeta-2)F' + 2\zeta(21\zeta-11)F'' + 8\zeta^2(\zeta-1)F''',$$

in terms of the hypergeometric function $F = {}_2F_1$ and its first three derivatives. It can be shown that as $r \to 0$ and $r \to 1$, Eq. (A17) reduces to the proper limits, Eqs. (A4) and (A11), respectively.

Footnotes

1. E. H. Taylor and S. Datz, J. Chem. Phys., 23, 1711 (1955).
2. E. F. Greene, R. W. Roberts, and J. Ross, J. Chem. Phys., 32, 940 (1960).
3. N. F. Ramsey, Molecular Beams (Clarendon Press, Oxford, 1956), p. 20.
4. See, for example, R. D. Present, J. Chem. Phys., 31, 747 (1959); B. H. Mahan, J. Chem. Phys., 32, 362 (1960); and Reference 5.
5. M. A. Eliason and J. O. Hirschfelder, J. Chem. Phys., 30, 1426 (1959).
6. An extensive table of Laplace transforms is given by A. Erdelyi, et al, Tables of Integral Transforms (McGraw-Hill Book Company, Inc., New York, 1954), Vol. I, p. 127.
7. R. D. Present, Kinetic Theory of Gases (McGraw-Hill Book Company, Inc., New York, 1958) pp. 137, 153; see also Reference 5.
8. Wall, Hiller, and Mazur, J. Chem. Phys., 29, 255 (1958).
9. Tables of Probability Functions (Nat'l. Bureau of Standards, 1941), Vol. I.
10. Reference 6, pp. 137 and 387.
11. A. Erdelyi, et al, Higher Transcendental Functions (McGraw-Hill Book Company, Inc., New York, 1953), Vol. II, p. 133.
12. A special case in which z^2 becomes independent of θ occurs for perpendicular collisions of beams having the same average velocity: $\alpha_1 = \alpha_2$, or $T_2/T_1 = M_2/M_1$ (see the Appendix).

Footnotes (Continued-1)

12. (Continued)

$\mathcal{P}_r(\theta)$ in Eq. (22) then becomes simply proportional to the distribution for elastic scattering, regardless of the velocity dependence of the reaction cross section.

13. In such cases one could in principle fit the function $G(1/\alpha^2)$ in Eq. (15) to experiment and then employ an inverse Laplace transform to determine $\sigma(v)$ via Eq. (13). In practice, however, only a very crude indication of $\sigma(v)$ could be obtained without extremely accurate data. The problem is similar to that of inferring energy level spacings from measurements of thermodynamic functions as discussed by E. Blade and G. E. Kimball, J. Chem. Phys., 18, 626 (1950); and S. H. Bauer, ibid., 6, 403 (1938); 7, 1097 (1939).

14. For further discussion of the transformation between laboratory and CM scattering angles, see, for example, L. I. Schiff, Quantum Mechanics (McGraw-Hill Book Company, Inc., New York, 1949), pp. 96-100.

15. The ambiguities are not entirely removed even when it is possible to use essentially monoenergetic beams as there remain distributions in the internal energy of reactants and products.

16. $\Delta D_0^0 = 4.2 \pm 1.1$ kcal/mole, from A. G. Gaydon, Dissociation Energies (Chapman and Hall, London, 1953).

Footnotes (Continued-2)

17. See W. D. McGrath and R. G. W. Norrish, Z. physik Chem. (Frankfurt) 15, 245 (1958); J. C. Polyani, J. Chem. Phys., 31, 1338 (1959); and F. T. Smith, ibid., 1352 (1959).

18. The relation between the ratio σ_r/σ_e and the usual steric factor is discussed in Reference 1. In Figs. 3, 6, and 7 we have for convenience set $\sigma_r = \sigma_e = 1A^2$; multiplication of the ordinate by the proper value and the conversion factor 6.023×10^{-11} will give the rate constant in units of sec^{-1} $(moles/cc)^{-1}$.

19. The original analysis given in Reference 1 was based on Model A. The formulas used were incorrectly derived, but this did not lead to significant numerical errors except in the calculated centroid distributions of Figs. 10-13, the discussion of which is amended here.

20. Reference 11, pp. 5, 14, and 86.

21. E. Jahnke and F. Emde, Tables of Functions (Dover Publications, New York, 1945), p. 6.

22. Reference 6, P. 196, and Reference 11, Vol. I, pp. 135, 370, 373.

23. Reference 11, Vol. I, p. 56.

Table I. Attenuation functions.[a]

z	$F_A = F_0(z)$	$F_B = F_0(z) - F_1(z)$	$(4/15)z^7 H'(z)$
0.00	1.0000-00	1.0000-00	0.0000-00
0.25	9.9999-01	9.8405-01	1.7253-05
0.50	9.9945-01	9.2421-01	1.8308-03
0.75	9.9255-01	8.1088-01	2.2886-02
1.00	9.1833-01	6.5164-01	1.1070-01
1.25	8.7320-01	4.7185-01	3.0075-01
1.50	7.2072-01	3.0407-01	5.4187-01
1.75	5.2523-01	1.7295-01	7.0740-01
2.00	3.3259-01	8.6358-02	7.0543-01
2.25	1.8160-01	3.7747-02	5.5601-01
2.50	8.5270-02	1.4420-02	3.5453-01
2.75	3.4430.02	4.8121-03	1.8595-01
3.00	1.1970-02	1.4027-03	8.1211-02
3.25	3.5895-03	3.5728-04	2.9811-02
3.50	9.3020-04	7.9554-05	9.2638-03
3.75	2.0871-04	1.5494-05	2.4679-03
4.00	4.0615-05	2.6411-06	5.5478-04
4.25	6.8660-06	3.9426-07	1.0782-04
4.50	1.0097-06	5.1566-08	1.8049-05
4.75	1.2933-07	5.9123-09	2.6092-06
5.00	1.4445-08	5.9457-10	3.2648-07

[a] For definitions, see Eqs. (25) and (29) of the text. The last two digits of each number in the table are the (negative) power of ten to be attached.

Table II. Conditions of a typical experiment: crossed beams of K(837°K) and HBr(460°K) intersecting at $\gamma = 90°$.

	Elastic collisions	Reactive collisions[a]
	"Most probable" initial conditions	
v_K	5.92×10^4 cm/sec	9.22
v_{HBr}	3.10	3.50
c	2.80	3.88
v	6.70	9.85
θ	47.6°	37.6°
ψ	27.9°	21.1°

	Comparison of possible final states			
	Q = 0	Q = -1	Q = 0	Q = 5 kcal
v_3'	2.23×10^4 cm/sec	0.37	0.52	0.69
v_4'	4.46	41.3	50.4	66.1
x_3	1.29	11.3	7.4	5.6
x_4	0.65	0.095	0.062	0.047
ϕ_3^{max}	50.90	5.1°	7.8°	10.2°
Eq. (38)	18.5% of 4π	0.20%	0.46%	0.79%
	3↔HBr; 4↔K	3↔KBr; 4↔H		

[a]The relative energy is taken as E = 3.0 kcal/mole, for which the most probable value of E_c is 2.2 kcal/mole.

Table III. Parameters for various reaction models.

Model	Cross Section Above E^*	E^* kcal/mole	σ_r/σ_e
A	σ_r	3.25 ± 0.12	1.34×10^{-2} ± 5%
B	$\sigma_r[1-(E^*/E)]$	2.51 ± 0.12	2.47×10^{-2} ± 5%
A-B	$\sigma_r(E^*/E)$	3.48 ± 0.08	2.01×10^{-2} ± 5%
C	$\sigma_r(E^*/E)^{10}$	3.97 ± 0.11	9.14×10^{-2} ± 5%

Captions for Figures

Fig. 1 Relations among initial velocity vectors.

Fig. 2 Attenuation functions corresponding to various values of n in Eq. (24). The insert shows the cross section functions for the three reaction models discussed in the text.

Fig. 3 Angular distribution of centroids in elastic scattering, for various angles of intersection of the beams.

Fig. 4 Variation of the activation energy parameter, z^2, with centroid angle θ for various angles of intersection of the beams.

Fig. 5 Angular dependence of the attenuation factor (a) for Model B, with $E^* = 3.0$ kcal/mole and various angles of intersection of the beams; (b) for Model C, with $\gamma = 90°$ and various values of the activation energy (kcal/mole).

Fig. 6 Angular distribution of centroids for reactive scattering; the conditions assumed correspond to those of parts (a) and (b) of Fig. 5.

Fig. 7 Dependence of rate constants for elastic and reactive scattering ($E^* = 3.0$ kcal/mole used) on the angle of intersection of the beams.

Fig. 8 Relation between the velocity vector of a product molecule M_3 as observed in the laboratory and in the center-of-mass reference system (primed); as indicated, the possible directions of v_3' generate a sphere.

Captions for Figures (Continued)

Fig. 9 Comparison of observed KBr distribution with calculated distribution of centroids for Model B. The curves are normalized to unit area. Experimental conditions are as in Table II, and E^* (kcal/mole) is taken as a parameter.

Fig. 1

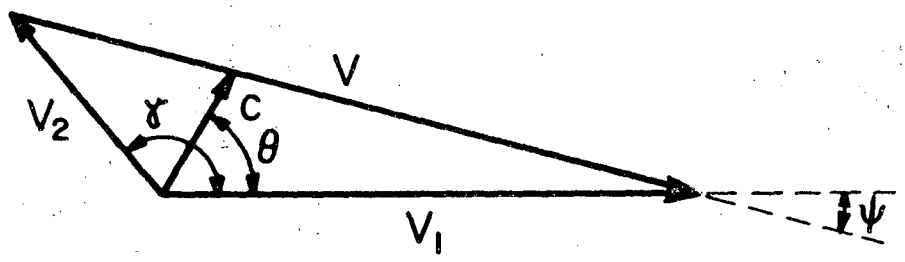

52.881-1

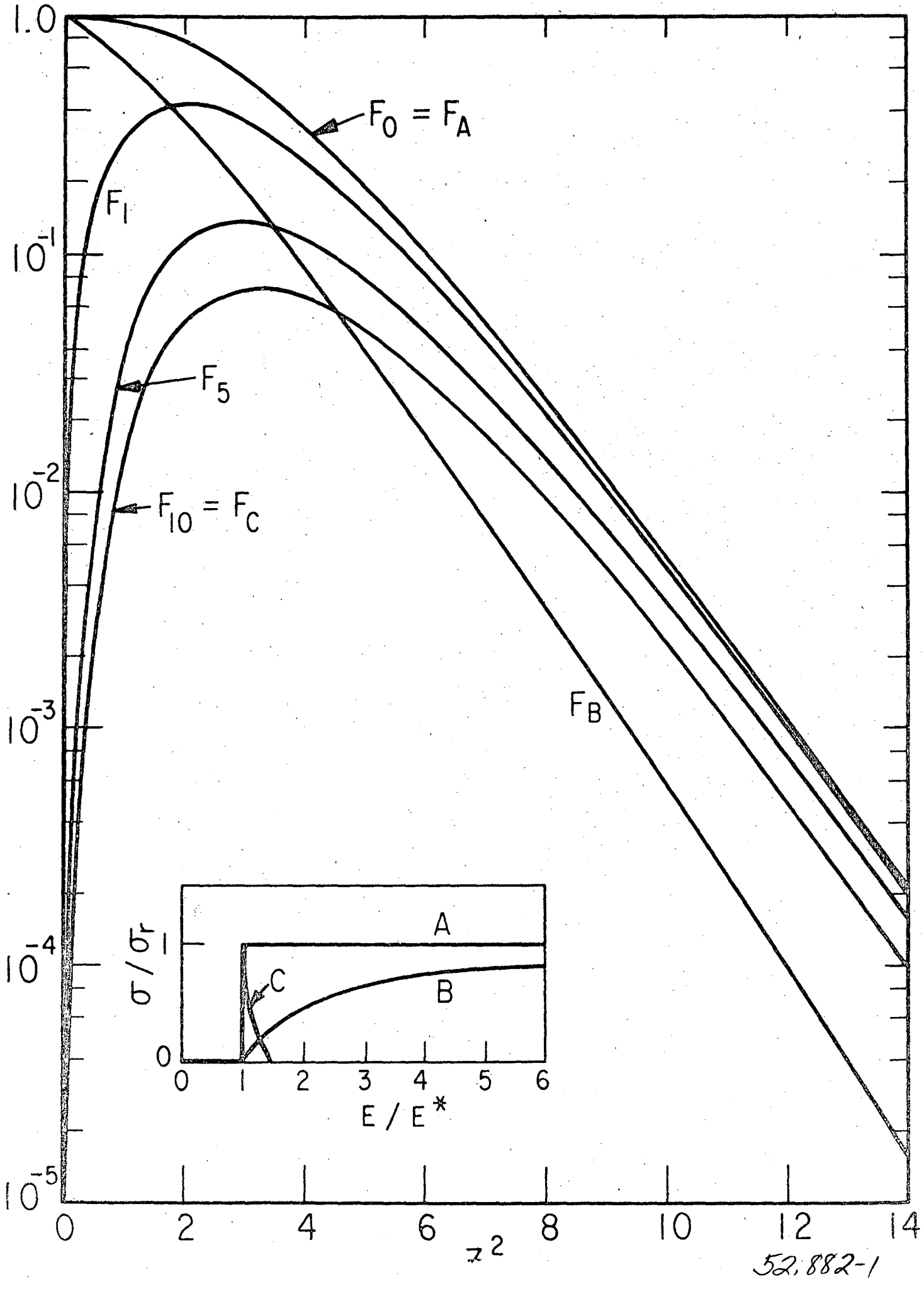
1.0
10^{-1}
10^{-2}
10^{-3}
10^{-4}
10^{-5}
$F_0 = F_A$
F_1
F_5
$F_{10} = F_C$
F_B
0
2
4
6
8
10
12
14
z^2
σ / σ_r
1
0
A
B
C
0
1
2
3
4
5
6
E / E^*
52,882-1

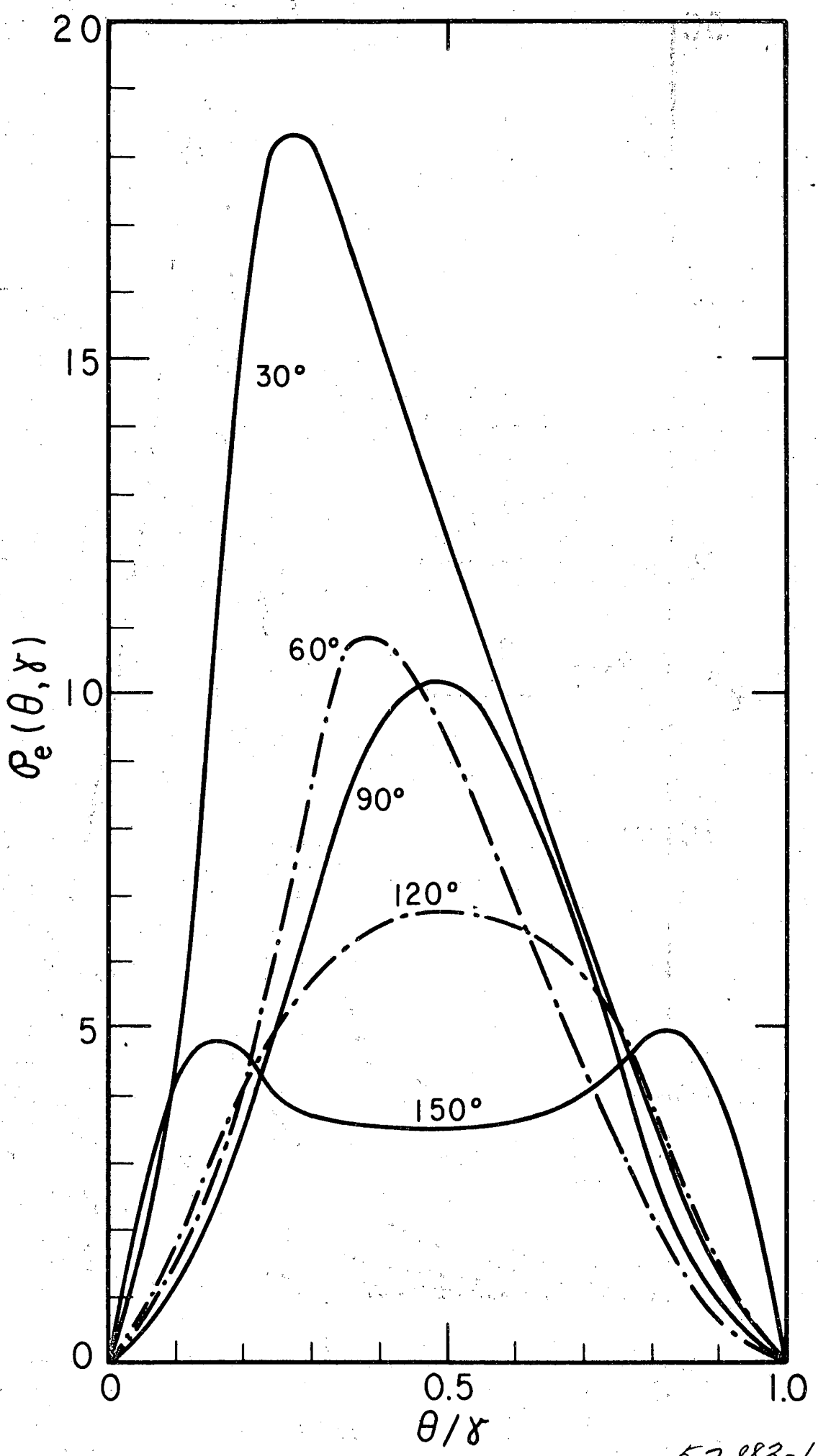
20
15
10
5
0
$\mathcal{P}_e(\theta,\gamma)$
30°
60°
90°
120°
150°
0
0.5
1.0
θ/γ

52.883-1

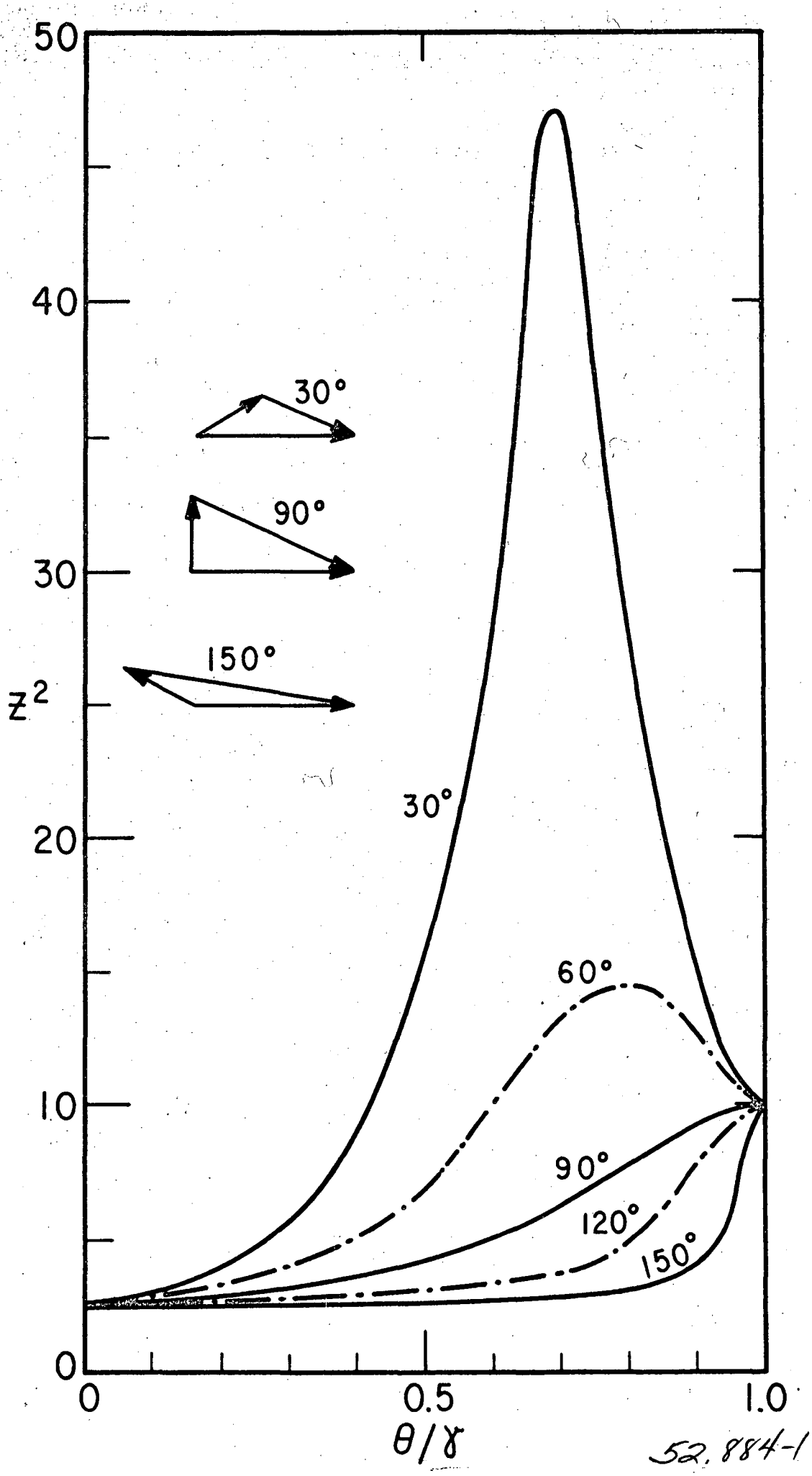

52,884-1

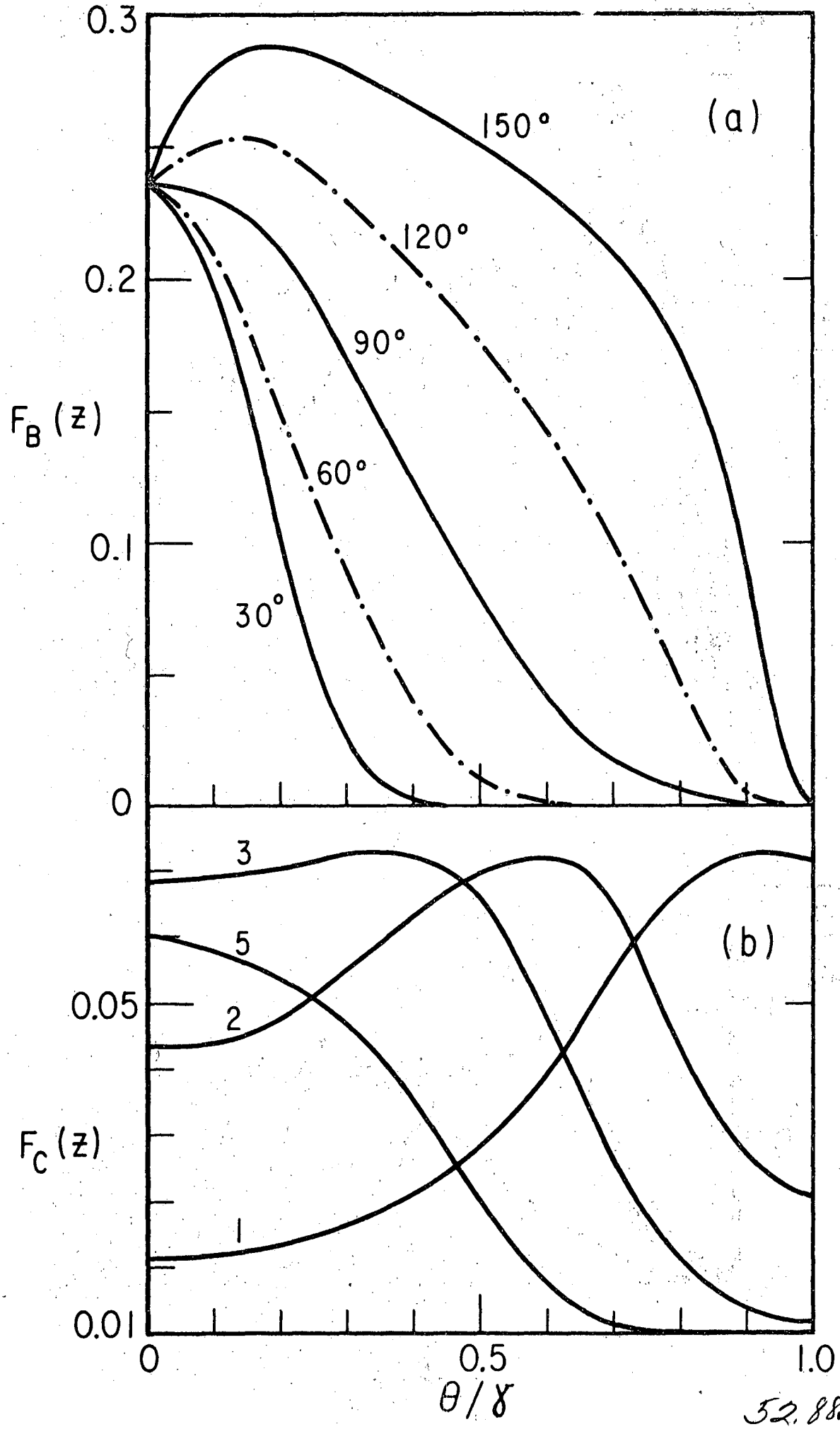
0.3
0.2
0.1
0
$F_B(z)$
150°
120°
90°
60°
30°
(a)
3
5
2
1
(b)
0.05
0.01
$F_C(z)$
0
0.5
1.0
θ/γ

52.885-1

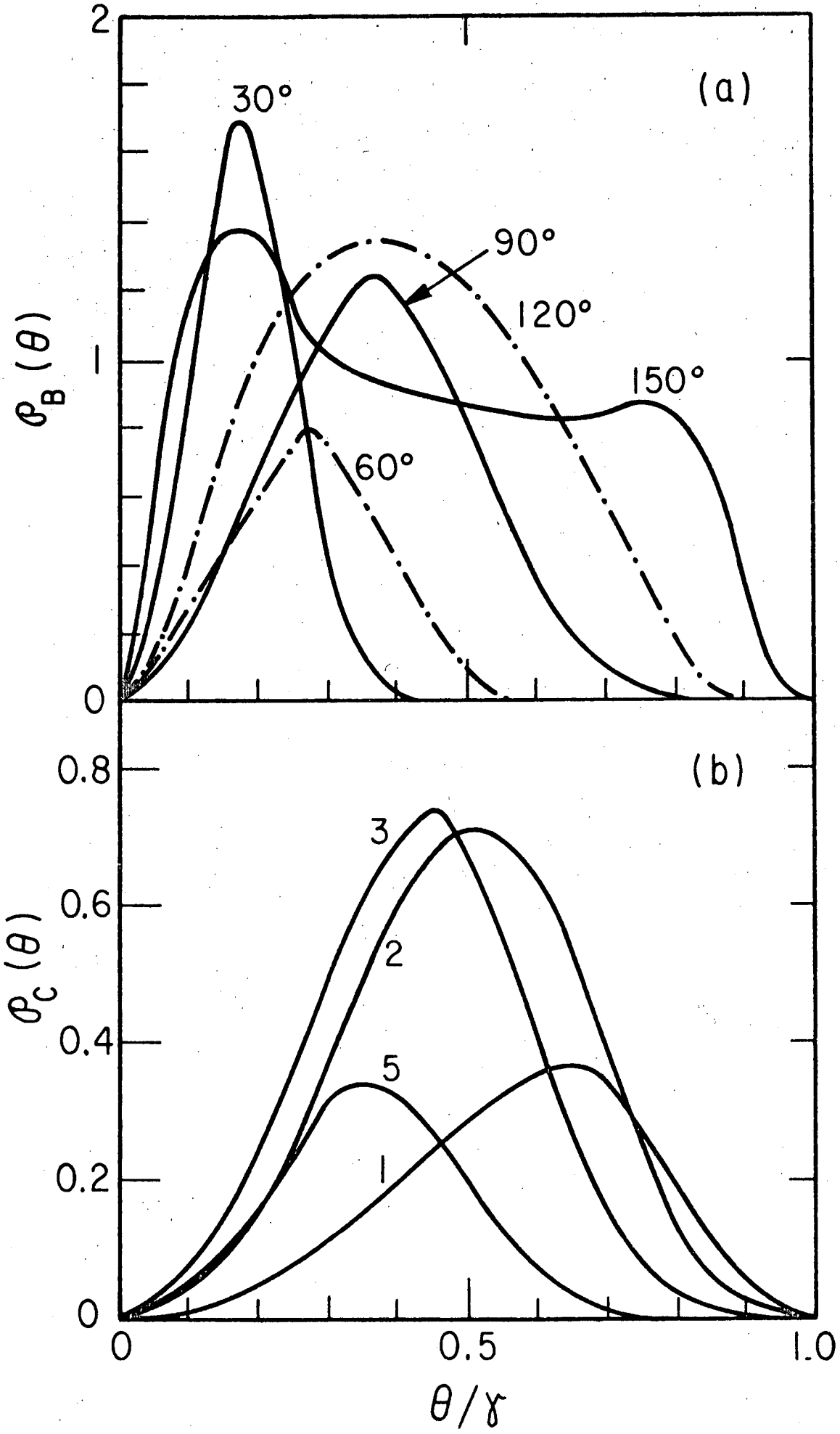
(a)
30°
90°
120°
150°
60°
$\mathcal{P}_B(\theta)$
2
1
0
(b)
3
2
5
1
$\mathcal{P}_C(\theta)$
0.8
0.6
0.4
0.2
0
0
0.5
1.0
θ/γ

52,886-1

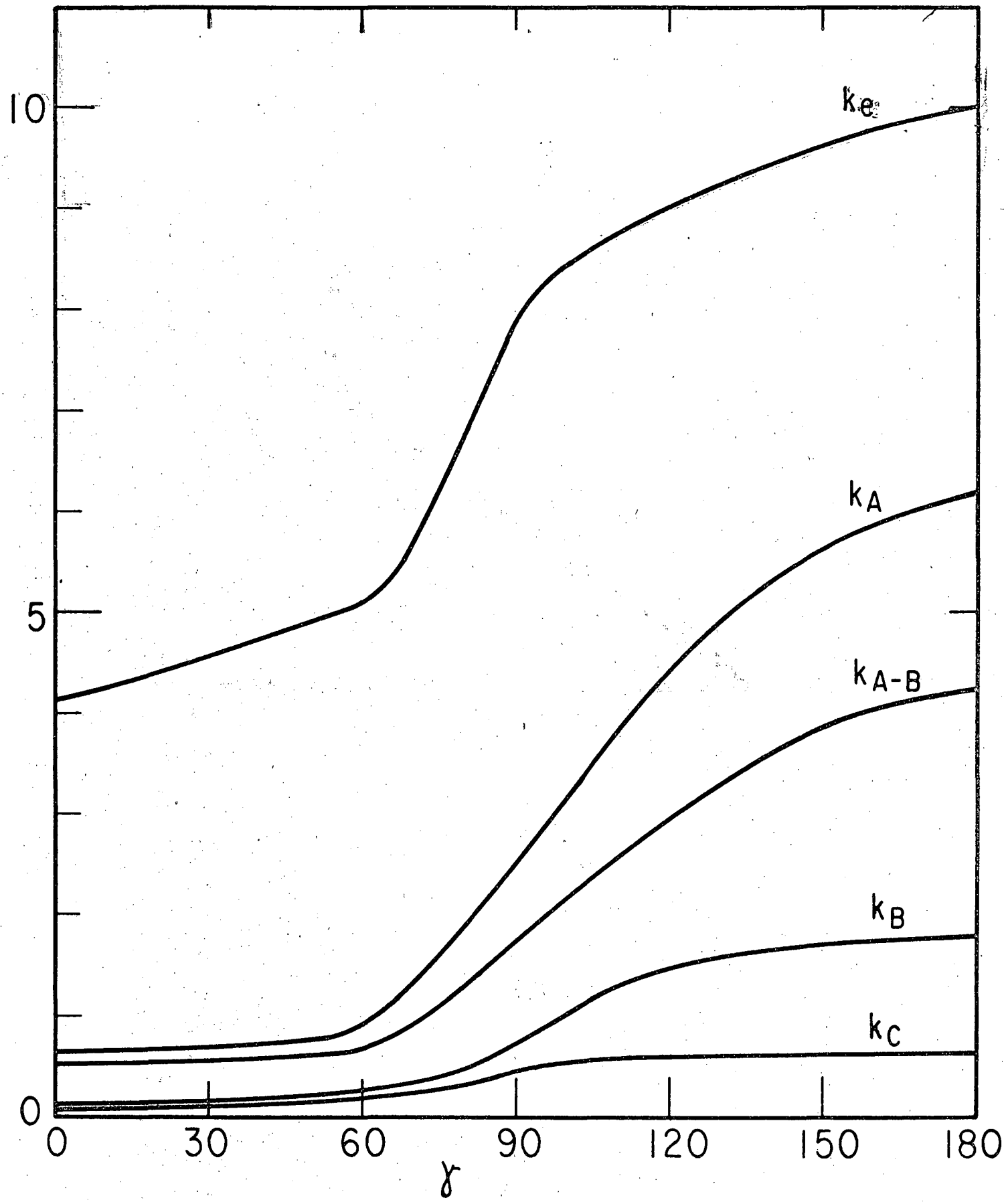

52,887-1

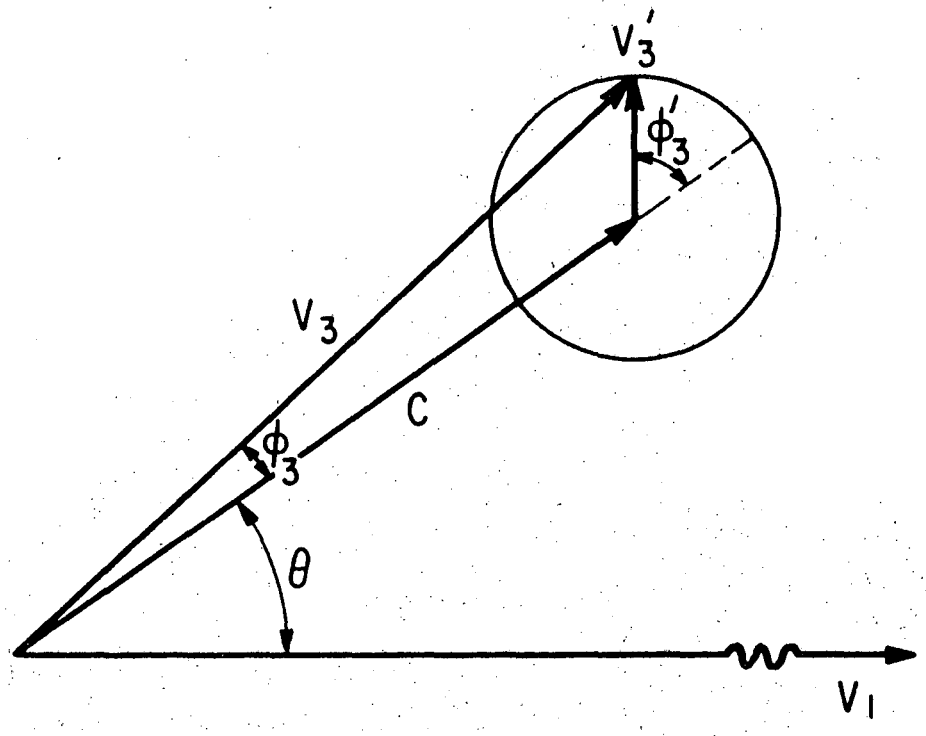

52,888-1

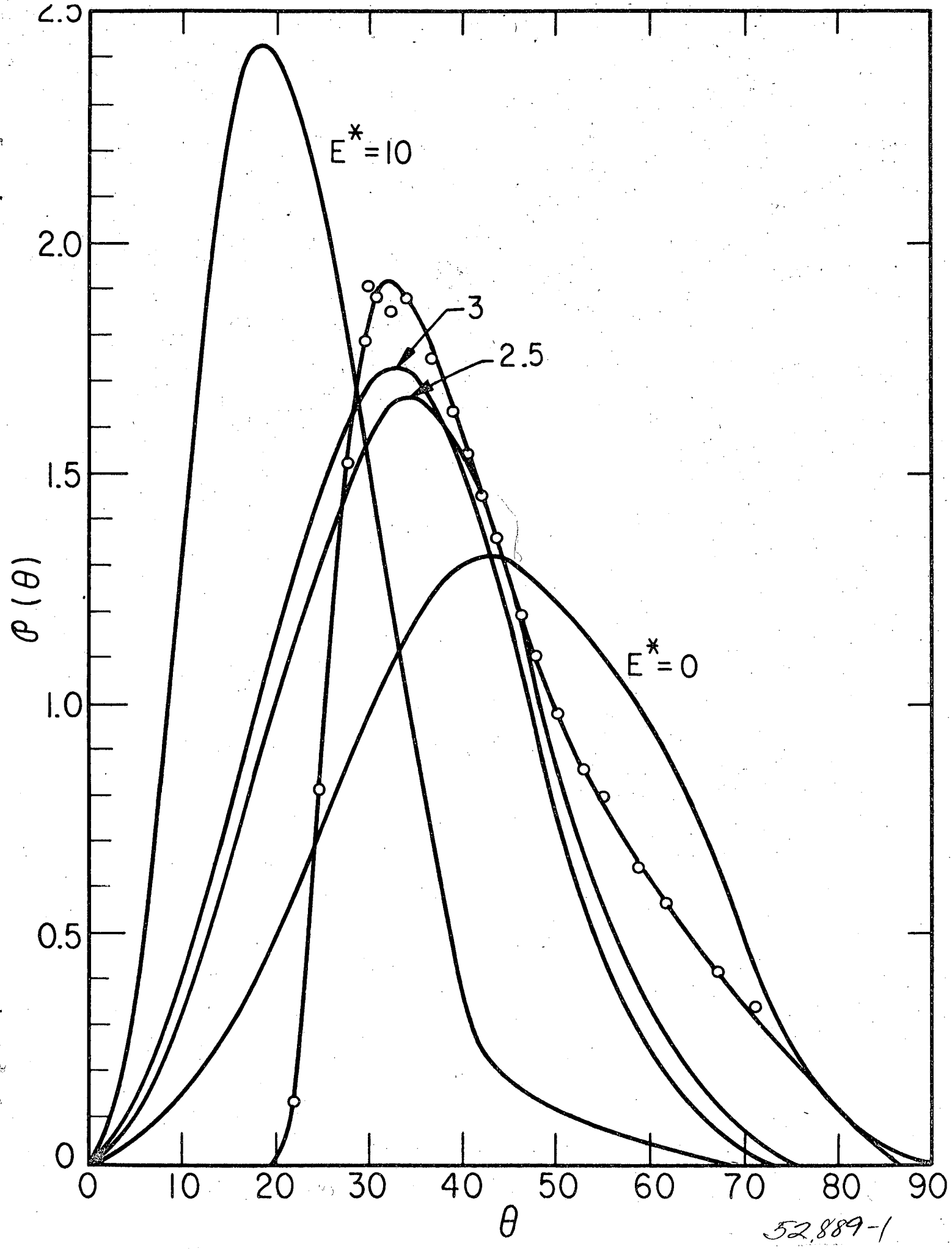
2.5
2.0
1.5
1.0
0.5
0
$\mathcal{P}(\theta)$
0
10
20
30
40
50
60
70
80
90
θ
$E^* = 10$
3
2.5
$E^* = 0$

52,889-1

This report was prepared as an account of Government sponsored work. Neither the United States, nor the Commission, nor any person acting on behalf of the Commission:

A. Makes any warranty or representation, expressed or implied, with respect to the accuracy, completeness, or usefulness of the information contained in this report, or that the use of any information, apparatus, method, or process disclosed in this report may not infringe privately owned rights; or

B. Assumes any liabilities with respect to the use of, or for damages resulting from the use of any information, apparatus, method, or process disclosed in this report.

As used in the above, "person acting on behalf of the Commission" includes any employee or contractor of the Commission, or employee of such contractor, to the extent that such employee or contractor of the Commission, or employee of such contractor prepares, disseminates, or provides access to, any information pursuant to his employment or contract with the Commission, or his employment with such contractor.